Computers and Chemical Engineering 160 (2022) 107740

Contents lists available at ScienceDirect

Computers and Chemical Engineering

journal homepage: www.elsevier.com/locate/compchemeng

Multiscale modeling of the microbial production of polyhydroxyalkanoates using two carbon sources

Stefanie Duvigneau[a,*], Robert Dürr[b], Michael Wulkow[c], Achim Kienle[a,d]

[a] Otto von Guericke University, Universitätsplatz 2, Magdeburg 39106, Saxony-Anhalt, Germany
[b] Magdeburg-Stendal University of Applied Sciences, Breitscheidsstraße 2, Magdeburg 39114, Saxony-Anhalt, Germany
[c] Dr. M. Wulkow Computing in Technology GmbH (CiT), Harry-Wilters-Ring 27, Rastede 26180, Lower Saxony, Germany
[d] Max Planck Institute for Dynamics of Complex Technical Systems, Sandtorstraße 1, Magdeburg 39106, Saxony-Anhalt, Germany

ARTICLE INFO

Article history:
Received 29 October 2021
Accepted 16 February 2022
Available online 20 February 2022

Keywords:
PHA production in bacteria
Population balance modeling
Polymerization kinetics
Hybrid cybernetic modeling
Chain length distribution

ABSTRACT

Polyhydroxyalkanoates are a promising material for a broad range of plastic products. Due to the high production costs, the proportion of industrial produced polyhydroxyalkanoates is low compared to conventional plastics. One possibility to reduce the costs is to reduce the price of the substrates using organic carbon-rich wastes streams. Using mathematical modeling, the microbial production process can be optimized by adjusting process conditions like the oxygen supply or initial substrate ratios. This contribution outlines a multiscale model for the poly(3-hydroxybutyrate) production in *Cupriavidus necator* using the carbon-sources fructose and acetate. The model comprises a hybrid cybernetic model to describe the macroscopic dynamics and a polymerization model which describes the chain length dynamics. The multiscale model is used to analyze the effects of different initial carbon to ammonium ratios and dissolved oxygen levels on the poly(3-hydroxybutyrate) concentration and chain length distribution.

1. Introduction

Polyhydroxyalkanoates (PHAs) are biopolymers that have a number of beneficial properties from an ecological point of view. PHAs are degradable in the environment and they can be produced microbially using wide variety of inexpensive substrates. As a result, no fossil fuels are required for the production. In addition, PHAs are biocompatible and non-toxic, which allows a large number of possible applications (Bugnicourt et al., 2014). Unfortunately, the production yields remain significantly behind those of conventional petroleum-based plastic production and the process is relatively costly in comparison to the established process (da Cruz Pradella, 2020).

In order to make the PHA process economically more competitive, many research is focused on process optimization strategies. For example, the use of inexpensive (or even free) substrates, such as waste animal fats, can not only make the process cheaper due to the free available substrate, but also reveal new, advantageous conditions for maximizing the PHA yield (Riedel et al., 2015). Further approaches for the use of waste feedstocks are summarized in the reviews (Tsang et al., 2019; Koller and Braunegg, 2018) and impressively show the diversity of the production process by only looking at the different substrates. In addition to minimizing the costs for the substrate, different process modes as well as mixed cultures are also investigated experimentally in order to increase bio-plastic production (Lopar et al., 2013; Sabapathy et al., 2020).

In order to save time and costs for experimental investigations, mathematical models can be used for analysis, for example to evaluate suitable process or substrate conditions (Jiang et al., 2011; Wang et al., 2007; Chatzidoukas et al., 2013). Conventional kinetic models neglect regulation and aim at a global description of substrate consumption and product yield dynamics (Scandola et al., 1998; Dias et al., 2005; Koller et al., 2006). In contrast, cybernetic modeling accounts for intracellular regulation, in particular optimal regulation in view of available resources is assumed. Hybrid cybernetic models (HCMs) combine cybernetic modeling and

Abbreviations: AM, active mode; CLD, chain length distribution; CN, carbon to ammonium ratio; DAE, differential algebraic equation; DO, dissolved oxygen; EM, elementary mode; ESS, normalized error square sum; GM, generating mode; HB, monomer unit of poly(3-hydroxybutyrate); HCM, hybrid cybernetic model; HPLC, high performance liquid chromatography; MW, molecular weight; PDI, polydispersity index; PHA, polyhydroxyalkanoate; PHB, poly(3-hydroxybutyrate); PHBV, poly(3-hydroxybutyrate-co-3-hydroxyvalerate); TBM, total biomass.

* Corresponding author.
E-mail address: stefanie.duvigneau@ovgu.de (S. Duvigneau).

https://doi.org/10.1016/j.compchemeng.2022.107740

Table 1
Cultivation conditions.

Data set	[FRU(0), ACE(0), NH_4Cl(0)] in g/L	DO	Cultivation	Volume
I	[22, 0, 1.7]	70%	bioreactor	1.2 L
II	[26, 4.4, 1.4]	5%	bioreactor	1 L
III	[0, 9.94, 1.4]	70%[a]	shake flask	0.2 L

[a] Assumed as controlled aerob cultivation with 70% dissolved oxygen (DO).

metabolic flux analysis in a systematic way (Ramkrishna and Song, 2018; Song et al., 2009a).

An HCM approach was also used in the present paper to simulate the substrate and product processes. Here, the homopolymer poly(3-hydroxybutyrate) (PHB) was produced in *Cupriavidus necator* using fructose and acetate, two carbon sources that occur in waste streams from e.g. juice or wine production. However, since it is not just the pure yield but also other polymeric properties, like medium chain length and polydispersity that determine the price of the polymer, model approaches should also take these into account.

With the chain length distribution (CLD) physical properties of the produced polymer can be concluded (Krevelen and te Nijenhuis, 2009). The first model approaches to describe the polymerization of PHB were developed by the research groups around Srienc and later Kiparissides (Mantzaris et al., 2001; 2002; Saliakas et al., 2007; Roussos and Kiparissides, 2012; Penloglou et al., 2010; 2012a; 2012b; 2017; Kiparissides, 2004). A simplified approach for the simulation of the CLD was also used in the present article (Dürr et al., 2021) and coupled with the recently published HCM (Duvigneau et al., 2021c). In contrast to the model in Penloglou et al. (2010), intracellular regulation was taken into account due to the HCM approach. In addition to the dynamics of substrates and product concentration, with the polymerization approach it is now possible to observe the CLD over time and to determine the characteristic variables of the distribution which affect polymeric properties, like weight average molecular weight (MW), within the production process.

In the present work, the dynamic behavior of the PHB CLD is simulated in a setup using the carbon sources fructose and acetate and ammonium chloride as nitrogen source. Here, disturbances caused by substrate pulses are considered in the simulations. In addition, we use the approach to predict the PHB yield and the CLD with the corresponding characteristic values at different dissolved oxygen (DO) concentrations and carbon to ammonium (CN) ratios. It is already known that the availability of oxygen has an influence on PHB production (Pratt et al., 2012), and our approach now additionally allows to investigate the composition of the produced polymer chains without additional measurements. With the characteristic values of the CLD such as weight average MW, number average MW or polydispersity index (PDI), material properties can be inferred and with that, explore possible application fields.

2. Experimental methods

2.1. Overview data sets and experimental setting

For the parameter identification of the hybrid cybernetic model three experimental data sets were used. The cultivation and initial conditions of each data set are given in Table 1. The analytical procedures to obtain substrate concentrations, PHB and biomass are described in the following sections. All experiments were performed with *Cupriavidus necator* (H16, DSM 428) obtained from DSMZ GmbH Braunschweig in M81 media at a constant temperature of 30 °C and pH 6.8. Bioreactor cultivations were performed in a DASGIP parallel bioreactor system (Eppendorf, Jülich). Before starting the main cultivation in the bioreactor, the bacteria were precultured at 30 °C and 150 rpm with 10 vol% filled 1 L shake flasks with the same initial substrates as supplemented in the main cultivation (see data set I + II in Table 1). For the experiment with acetate as single carbon source (data set III) 1 L shake flasks was filled with 200 mL culture and incubated at 30 °C and 150 rpm for 120 h.

2.2. Substrate concentration

For the determination of all substrate concentrations the supernatant after centrifugation of the biomass was used. The substrate acetate was obtained with an Agilent 1100 high performance liquid chromatography (HPLC). For this, the supernatants of each sample were filtered trough a 0.2 μm nylon membrane. After that, 10 μL of the filtered supernatants were loaded on a reversed phase column (Inertsil 100A ODS-3, 5 μm pore size, 250 × 4.6 mm, MZ-Analysentechnik GmbH, Mainz, Germany) and eluted isocratically with 1 mL min^{-1} and 0.1 M $NH_4H_2PO_4$ at pH 2.6 and 40 °C. The ammonium concentrations were determined using an enzymatic test kit (Kit No. 5390, R-Biopharm AG, Darmstadt, Germany) and following the manufactures instructions. For data set II, fructose concentrations were determined by HPLC by loading 10 μL of the filtered supernatants on a RHM monosaccharide column (Phenomenex, Torrance, USA) and eluted isocratically with 0.6 mL min^{-1} deionidized water. The column oven was heated to 80 °C and the refractive index detector was tempered to 60 °C. The fructose concentrations of the other two data sets were determined using the enzymatic test kit (Kit No. 10139106035, R-Biopharm AG, Darmstadt, Germany) and following the manufactures instructions.

2.3. Polyhydroxybutyrate concentration

Concentrations of hydroxybutyrate (HB) in the PHB polymer were determined applying the procedure published in Duvigneau et al. (2021c) using an Agilent 1260 HPLC. For this, 1 mL of the culture broth was alkaline digested as reported in Satoh et al. (2016). The samples were filtered through a 0.2 μm nylon membrane and 10 μL were loaded on the reversed phase column (Inertsil 100A ODS-3, 5 μm poresize, 250 × 4.6 mm, MZ-Analysentechnik GmbH, Mainz, Germany) and eluted isocratically with 1 mL min^{-1} at 60 °C with 92% low concentrated H_2SO_4 (0.025% solution, Carl Roth, Karlsruhe) and 8% acetonitrile (Carl Roth, Karlsruhe). Detection was performed with a photodiode-array detector (G7115A, Agilent,Waldbronn, Germany) at 210 nm. The 3HB concentrations in the polymer chains of the samples were determined by using crotonic acid (Carl Roth, Karlsruhe, Germany). In parallel, a poly(3-hydroxybutyrate-co-3-hydroxyvalerate) sample (12% 3-Hydroxyvalerate, Sigma-Aldrich /Merck, Darmstadt, Germany) with known concentration was measured to calculate the conversion yields as described in Duvigneau et al. (2021c).

2.4. Determination of biomass

For the determination of total biomass (TBM), 1 ml of culture broth was collected and centrifuged for 10 min at 9600 × *g* and 4 °C (VWR MicroStar 17R, Pennsylvania, USA). After that, the cell pellet was dried over night at 80 °C and weighted.

3. Mathematical modeling

The developed metabolic framework includes two parts: a hybrid cybernetic and a polymerization model. For the setup of the HCM a metabolic model is necessary, that can be reduced using metabolic yield analysis (Song and Ramkrishna, 2009). This is explained in the next section. In contrast, the polymerization model

accounts for the dynamics of the CLD (see Section 3.3). Both models are coupled and thus coupling conditions must be given to build a linkage between HCM and polymerization kinetics (see Section 3.4). Finally, numerical solution of the coupled model is discussed in Section 3.5.

3.1. Metabolic model and yield analysis

The metabolic model published in Franz et al. (2011) was updated using the data base *KEGG* (KEG, 2020) and extended by the consumption of acetate as shown in Yu and Si (2004). The resulting metabolic model used in this work was first presented in Duvigneau et al. (2020). The metabolic reactions are shown in Appendix A.

To use the stoichiometric information of the metabolic model in a hybrid cybernetic modeling approach, a suitable subset of reactions to describe the conversion from substrates to products is necessary. The sets of reactions explaining the consumption of a certain substrate to produce, e.g. biomass or PHB, are called elementary modes (EMs). EMs of our metabolic model were calculated using the program *Metatool 5.1* (Metatool, 2019), resulting in a total number of 4857 EMs. In a next step, the calculated EMs need to be classified into different sub-models according to the input substrates in order to keep functionality of the overall model. This procedure was suggested in Song et al. (2009a) for the first time and was also used for our case. After the definition of submodels the *MATLAB* command *convhulln* can be used to design the convex hull in yield space for each of the sub-models. The convex hull is spanned by generating modes (GMs), which is defined as the relevant set of EMs of each submodel to describe process dynamics. For further information regarding the analysis in yield space we refer to the publication of Song and Ramkrishna (2009). For the presented model, 38 GMs were selected to describe the process dynamics.

In a next step, further reduction takes place by selecting active modes (AMs) relevant to experimental data. The selection of AMs was done during the estimation of the parameters $k_{r,i}$ (explanation in the next section). With that, the set of GMs with the smallest normalized error square sum (ESS, (1)) was chosen as AM set used in the HCM.

$$ESS = \sum_{i=1}^{n} \left(\frac{\mathbf{x_{exp}}(t_i) - \mathbf{x_{sim}}(\mathbf{t_i})}{\max(\mathbf{x_{exp}})} \right)^2 \tag{1}$$

The differences between n simulated and experimental data points (x_{sim} and x_{exp}) at time t_i were used to calculate the ESS. The ESS is weighted with the corresponding maximum experimental value. The vector $\mathbf{x}$ is defined as $\mathbf{x} = \left[c_{fru},\ c_{ace},\ c_N,\ x_{HB},\ c\right]$.

3.2. Hybrid cybernetic model

The dynamics for the fructose (c_{fru}), acetate (c_{ace}) and ammonium (c_N) concentrations, the HB proportion of the total biomass $\mathrm{x_{HB}}$ and the total biomass concentration c can be described by the following ordinary differential equations:

$$\frac{d}{dt}\begin{bmatrix} c_{fru} \\ c_{ace} \\ c_N \end{bmatrix} = \mathbf{S_s Z r_M} \mathrm{c}\,, \qquad \frac{\mathrm{dx_{HB}}}{\mathrm{dt}} = \mathbf{S_{HB} Z r_M}\,, \qquad \frac{\mathrm{dc}}{\mathrm{dt}} = \mu \mathrm{c}\,. \tag{2}$$

The AM matrix in yield space for the substrates $\mathbf{S_S Z}$ was determined as described in the previous section. The values can be seen in Table B.1. The influence of substrate availability in the ith AM can be expressed by the kinetic $r_{M,i}$:

$$r_{M,i} = v_i k_{r,i} e_i^{\mathrm{rel}} r_{\mathrm{core,i}}\,. \tag{3}$$

The relative enzyme level e_i^{rel} of the ith AM is given in Eq. 7. The rate $r_{\mathrm{core,i}}$ of the ith AM is a Monod-type kinetic consisting of math fractions for n consumed substrates s:

$$r_{core,i} = \frac{s_1}{K_{s_1} + s_1} \cdot \cdots \cdot \frac{s_n}{K_{s_n} + s_n}. \tag{4}$$

The hybrid cybernetic control variable v_i describes enzyme activity of the ith AM and can be calculated as shown in Eq. (9). The parameters $\mathbf{k_r}$ for every AM can be found in Table B.2.

In order to use the metabolic information within the HCM, it is assumed that substrates and products have slow dynamics in comparison to internal metabolites and intermediates. For that reason, dynamics of the latter can be neglected and no model equations are needed for them. To describe the dynamics of biomass production using metabolic information, a definition for the growth rate μ with the rate vector $\mathbf{r_M}$, the AM vector $\mathbf{S_c Z}$ (row 5 in Table B.1) for biomass production and an oxygen-dependent factor K_μ is necessary.

$$\mu = \mathbf{S_c Z r_M} K_\mu \tag{5}$$

The oxygen-dependent factor K_μ describes the proportion between the growth rate of a certain DO level and the growth rate applying aerobic conditions with a DO of 70%:

$$K_\mu = \frac{\mu(\mathrm{pO_2})}{\mu(70\%)} \quad \text{with} \quad \mu(pO2) = -0.151\ \mathrm{pO_2} + 0.256\,. \tag{6}$$

The linear equation $\mu(pO2)$ was developed with multiple datasets from our lab (unpublished data). With the introduction of the factor K_μ it is possible to introduce data sets with different oxygen availability and investigate the process behavior at different DO levels.

Beside the description of the substrate and product dynamics differential equations for enzymes of each AM are given as follows

$$\frac{d\mathbf{e}}{dt} = \alpha + \mathbf{r_{EM}} b - \beta \mathbf{e}\,, \text{ where } e_i^{\mathrm{rel}} = \frac{e_i}{e_i^{\max}} \text{ with } e_i^{\max} = \frac{\alpha_i + k_{e,i}}{\beta_i + k_{r,i}(\mathbf{S_c Z})_\mathbf{i}}\,. \tag{7}$$

The enzyme levels increase with a constitutive enzyme synthesis rate α and the enzyme synthesis due to metabolic activity $b = 1 - x_{\mathrm{PHB}}$ (second term). Enzyme degradation by a protein turnover (β) is given in the third term $-\beta\mathbf{e}$.

The kinetic rates r_{EM} describe the enzyme synthesis due to metabolic activity and can be expressed for the ith AM as follows:

$$r_{EM,i} = u_i k_{e,i} r_{core,i.} \tag{8}$$

The rate $r_{\mathrm{core,i}}$ expresses the influence of all consumed substrates as shown in Eq. (4). The rate constants $\mathbf{k_e}$ for all AMs are given in Table B.2.

One major advantage of the HCM approach is the ability to describe intracellular regulation via enzyme synthesis and activity. For this, the hybrid cybernetic control variables for enzyme synthesis and activity $\mathbf{u}$ and $\mathbf{v}$ are introduced and calculated as described in (Young and Ramkrishna, 2007):

$$\mathbf{u} = \frac{\mathbf{p}}{\|\mathbf{p}\|_\mathbf{1}} \qquad \mathbf{v} = \frac{\mathbf{p}}{\|\mathbf{p}\|_\infty}. \tag{9}$$

The return on investment $\mathbf{p}$ can be calculated under the assumption that the bacteria always try to maximize carbon source uptake. With that objective, $\mathbf{p}$ can be defined as

$$\mathbf{p} = diag(\mathbf{f_c}) diag\left(\mathbf{e}^{rel}\right) diag(\mathbf{k_r}) \mathbf{r}_{core} \tag{10}$$

The vector of uptaken carbon units $\mathbf{f_c}$ is normalized by using the highest carbon uptake ($\mathbf{f_c}(1)$) and is illustrated in Table B.1.

3.3. Polymerization model

To account for the dynamics of the CLD, the HCM is complemented with a population balance model (Vale and McKenna, 2005). Here, polymers are distinguished into active (living) and inactive (dead) polymer species. The dynamics of their CLDs are described by

$$\begin{aligned}\frac{d\,[LP]_i}{d\,t} &= \underbrace{\delta(i-1)k_{ini}[HB\text{-}Syn]}_{initiation} + \underbrace{k_{m2}\,[HB]\left([LP]_{i-1}-[LP]_i\right)}_{propagation} - \underbrace{k_{term}[LP]_i}_{change}\\ \frac{d\,[DP]_i}{d\,t} &= \underbrace{k_{term}[LP]_i}_{change} - \underbrace{k_{dep}\left([DP]_i-[DP]_{i+1}\right)}_{degradation}\end{aligned} \tag{11}$$

where $[\circ]_i$ denotes the number density distribution of chains with distinct chain length i. Active polymer chains (LP) have the ability to elongate after initiation of initial chain with length $i = 1$. The corresponding rate constant is k_{ini}. Termination of living polymer chains of arbitrary length to inactive polymer chains (DP) with rate constant k_{term} is assumed to be independent of the chain length. Depolymerization, i.e. chain length shortening, can only take place on inactive polymer chains (DP). In contrast to Penloglou et al. (2017), the species of intermediate polymers is neglected in our formulation. The dynamics of the monomer concentration and the monomer-synthase complex are given by

$$\begin{aligned}\frac{d\,[HB]}{d\,t} &= -k_1[HB][Syn] - k_{m2}[HB]\sum_{i=1}^{\infty}[LP]_i + M^+,\\ \frac{d\,[HB\text{-}Syn]}{d\,t} &= k_1[HB][Syn] - k_{ini}[HB\text{-}Syn].\end{aligned} \tag{12}$$

The equations above describe the coupling of a first monomer [*HB*] to a synthase dimer complex [*Syn*] with the rate constant k_1. After successful attachment of the monomer to the enzyme complex, conversion to *LP* of length 1 takes place with k_{ini}. Furthermore, monomers are required to elongate active polymers LP with the rate constant k_{m2}. The monomer production rate M^+ represents the generation of new monomer units by metabolization of substrates. Further information is given in the next section.

With abundance of synthase dimer complexes [*Syn*] the first term in both equations reduces to

$$k_1[HB][Syn] = k_{m1}[HB]. \tag{13}$$

Furthermore, it is assumed that monomer units generated by depolymerization of the DPs are directly converted into biomass and thus do not flow back into the pool of monomers as described in the equation above. For later computational implementation those are defined as "dead" monomers [HB_{BIO}] and their overall balance is given as

$$\frac{\mathrm{d}\,[HB_{BIO}]}{\mathrm{d}\,t} = \sum_{i=1}^{\infty} k_{dep}[DP]_i. \tag{14}$$

All constant parameter values for the polymerization model are given in Table C.1

3.4. Coupling between HCM and polymerization model

As a matter of fact, the polymerization kinetics (11) and (12) can be implemented as an augmentation of the macroscopic metabolic model (2)–(10). Dynamics of the first depend on the dynamics of the latter and are coupled via the monomer production rate M^+, which must take values such that the overall model is consistent, i.e., the total concentration of PHB (concentration of all monomers HB in all chains) from the polymerization model has to match its counterpart predicted by the macroscopic model at all times. The corresponding algebraic condition reads as

$$\frac{1}{MW_{HB}} m_{HB} = \sum_{i=1}^{\infty} i([LP]_i + [DP]_i) \tag{15}$$

and the corresponding derivative as

$$\begin{aligned}\frac{1}{MW_{HB}}\frac{\mathrm{d}\,m_{HB}}{\mathrm{d}\,t} &= \frac{\mathrm{d}}{\mathrm{d}\,t}\left\{\sum_{i=1}^{\infty} i([LP]_i + [DP]_i)\right\}\\ &= k_{ini}[HB\text{-}Syn] + k_{m2}[HB]\sum_{i=1}^{\infty}[LP]_i - \underbrace{k_{dep}\sum_{i=1}^{\infty}[DP]_i}_{r_{HB}^- MW_{HB}{}^{-1}}.\end{aligned} \tag{16}$$

The degradation rate r_{HB}^- can be derived from the HCM. Using this rate, the depolymerization rate parameter k_{dep} for the polymerization model can be calculated with the molecular weight of a HB monomer (MW_{HB}=86 g/mol) as follows

$$k_{dep} = \frac{r_{HB}^-}{MW_{HB}\sum_{i=1}^{\infty}[DP]_i}. \tag{17}$$

In contrast to the model presented in Dürr et al. (2021), the current formulation omits steady state assumptions on the dynamics of monomers [*HB*] and monomer-synthase complex [*HB-Syn*] resulting in a differential algebraic system of equations for the combined polymerization and macroscopic model. The solution strategy is discussed in the next section.

3.5. Numerical solution approach

While the macroscopic HCM represents a rather low dimensional system of ODEs, the polymerization model represents a high dimensional ordinary differential equation system. In principle both models could be solved individually with appropriate numerical solution software, e.g., *Matlab2019b*, eventually after complexity reduction using (approximate) moment methods for the latter (Dürr and Bück, 2020). However, solution of the combined model formulation, i.e. macroscopic and polymerization dynamics, is more challenging. In fact, the overall multiscale model represents a differential algebraic equation (DAE) system. In our previous publication (Dürr et al., 2021), we chose a pragmatic solution approach based on steady-state assumptions of the monomer and the monomer-synthase complex. Thereby, the DAE system could be reduced to a set of ODEs.

In this contribution, we abstain from the steady-state assumption and follow an alternative approach described in the following: The complete model solution can also be viewed in terms of a control problem where a monomer production rate has to be determined as a feedback control law

$$M^+ = F(e_{HB}). \tag{18}$$

There, the error between the mass of PHB (mass of all HB monomers in all chains) predicted by the polymerization model, and the reference value, i.e. the mass of HB computed with the HCM,

$$e_{HB} = m_{HB} - MW_{HB}\sum_{i=1}^{\infty} i([LP]_i + [DP]_i) \tag{19}$$

is attenuated. Obviously, such an approach only represents the approximate solution of the underlying DAE. In principle, any controller could be chosen, however its dynamics have to be fast and reliable to provide a reasonably accurate approximate solution to

Table 2
Modules of the implemented PREDICI model. HB_{bio} is the amount of polymer converted to biomass caused by degradation of inactive polymers DP. Only active polymers (LP) can prolong.

Name	Reaction			Coefficient
Elemental reaction	HB	→	HB-Syn	k_{m1}
Initiation by decay	HB-Syn	→	LP(1)	k_{ini}
Propagation	LP(i) + HB	→	LP(i+1)	k_{m2}
Change	LP(i)	→	DP(i)	k_{term}
Degradation	DP(i)	→	DP(i-1) + HB_{bio}	k_{dep}
Extraction	DP(1)	→	HB_{bio}	k_{dep}

the DAE system. The probably most pragmatic solution for the design of the feedback law (18) is a PID control law

$$M^{+}(t) = K_P e_{HB}(t) + K_I \int_0^t e_{HB}(\tau)\mathrm{d}\tau + K_D \dot{e}_{HB}(t)\,. \tag{20}$$

With some manual or rule-based tuning of the parameters an accurate solution can be obtained. The controller complexity sufficient for the simulations in this paper is a P-controller, parameters are given in Table C.2. However, overall stability of the control system is generally not guaranteed and thus performance in terms of the control error has to be monitored closely. Due to the one-way coupling, the model solution was implemented as follows: At first, the macroscopic part (HCM) was solved in MATLAB. The resulting overall PHB masses were exported to PREDICI where the previously described polymerization model was implemented with the "feedback"-solution to guarantee matching between the two model types. More information about the implementation and solution in PREDICI is given in the next section.

3.6. Simulation of polymer systems in PREDICI

PREDICI (Wulkow, 2008) is a commercial software package for the general simulation of polymer kinetics and population balances with discrete or continuous property coordinates, in particular for chain-length distributions $P_i(t)$ (in the present context $[LP]_i$ and $[DP]_i$). These distributions are efficiently approximated on the chain-length axis (index i) by means of a self-adaptive Galerkin-hp-method. The Galerkin-FEM is connected to a special time loop that discretizes first in time and then on the property axis with grids that may vary from time step to time step for maximal adaptivity. The solved balances are entered in terms of modular reaction step patterns that allow arbitrary combinations. The system described in (11) and (12) consists of the reactions in Table 2.

The respective input in PREDICI principally leads to the equations shown in (11) and (12), but these are solved directly in the approximating space for any chain-length range. The treatment in PREDICI includes all side balances of monomers and reactor variables, in particular the closed mass balance, and also provides engineering operations like controllers.

Since in the present model the monomer balance - that is already connected to reaction steps - has to be controlled by the results of the MATLAB model, an additional differential equation for $[HB]$ has been added that in turn uses a controller (20). By that the monomer concentration is forced to be close to the path given by the PREDICI-external model. The results of the simulation are the full chain-length distributions given for each single chain length, i.e. $[LP]_i$ and $[DP]_i$ $(i = 1, 2, \ldots, \infty)$ and all variables that can be derived from them, in particular moments and important mean values.

3.7. Characteristic values of a chain length distribution

In this contribution, we compare three common characteristic values of the distribution $P_i(t)$: number average MW $(M_n^P(t))$, weight average MW $M_w^P(t)$ and polydispersity index (PDI). All of them can be calculated by using the zeroth, first and/or second statistical moment of the distribution. The general rule to calculate the kth moment for a general chain-length distribution $P_i(t)$ is:

$$\lambda_k^p(t) = \sum_{i=1}^{\infty} i^k \cdot P_i(t)\,. \tag{21}$$

The definitions for calculating the characteristic values of a distribution are:

$$M_n^P(t) = \frac{\lambda_1^p(t)}{\lambda_0^p(t)} \cdot M_M^P\,, \tag{22}$$

$$M_w^P(t) = \frac{\lambda_2^p(t)}{\lambda_1^p(t)} \cdot M_M^P\,, \tag{23}$$

$$\mathrm{PDI} = \frac{M_w^P(t)}{M_n^P(t)}\,. \tag{24}$$

The average molecular mass per monomer unit M_M^P corresponds to the molar mass of a monomer in case of producing polymers with unique monomers, e.g. the homopolymer PHB. For the presented model, the characteristic values are computed for the overall polymer, i.e., the sum of active and inactive polymer chains

$$P_i = [LP] + [DP]_i\,. \tag{25}$$

Note, that the first moments of the individual polymeric species $[LP]_i$ and $[DP]_i$ are already used in (15) and related balances.

4. Results

In the following, we apply the presented multiscale model approach to PHB production using fructose and acetate as carbon sources and ammonium chloride as nitrogen source. Once the nitrogen concentration is almost zero, PHB is accumulated in the cells by conversion of the given carbon sources. Disturbances such as an ammonium chloride shot or an increase of one or both carbon source concentrations introduced by the operator of the experimental plant were made to challenge the model with different biological behaviors.

In the following, we show and discuss the performance and outcomes of the two parts of the multiscale model. First, the macroscopic HCM is used to simulate the substrate and product dynamics from the above described experimental setting. Then, the setup was evaluated with regard to the CLD and their characteristic values using the polymerization model. Finally, we use our established model to investigate different CN ratios and DO levels on maximum PHB yield and the corresponding chain length distributions.

4.1. HCM simulation

In the first step, a kinetic model is required, which describes the degradation of substrates and the production of PHB and biomass on a macroscopic level. The simulation result for the concentration profiles using our recently published HCM can be seen in Fig. 1 (Duvigneau et al., 2021b). The model is able to qualitatively reflect the experimental data (diamond) for the substrate degradation, the polymer accumulation and non-PHB biomass growth. Additionally, the approach can account for pulsed substrate changes.

Next, the simulated macroscopic PHB concentration as well as the PHB consumption rates are extracted and loaded into the PREDICI as described in the previous section. To ensure the conservation of mass (Eq. (19)) of the two model parts, a controller

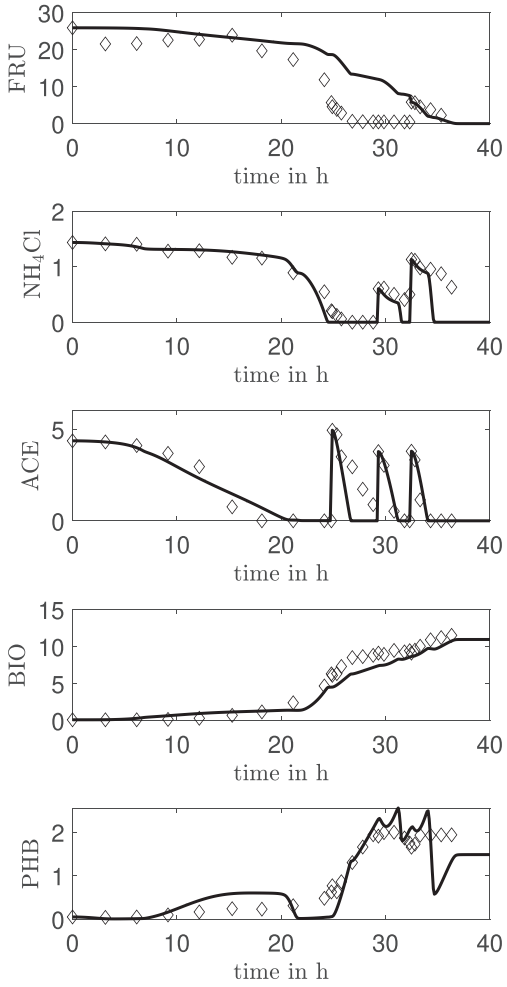

Fig. 1. Model simulation and experimental data set (fructose and acetate co-feeding, diamonds) using the HCM approach. Legend: FRU, fructose; NH_4Cl, ammonium chloride; ACE, acetate; BIO, total biomass; PHB, polyhydroxybutyrate. All concentrations are given in g/L.

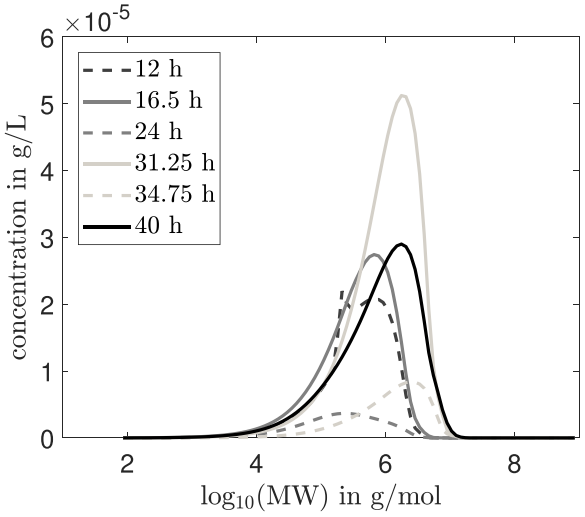

(a) Chain length distribution (CLD) of chosen time points (see legend).

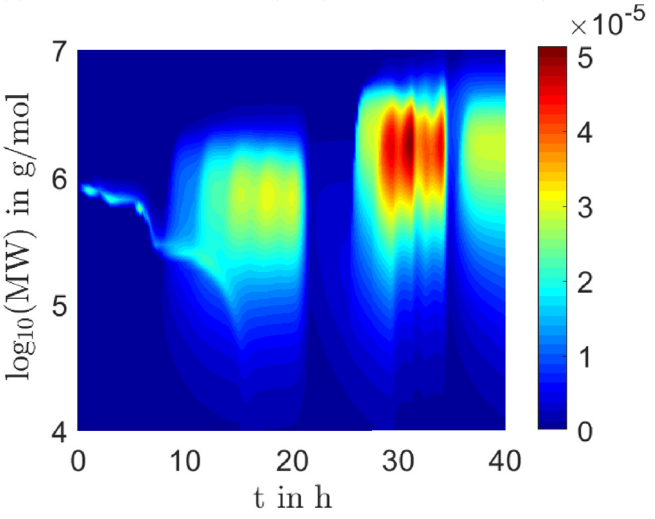

(b) Dynamics of the molecular weight distribution (color bar) over time and molecular weight of each chain.

Fig. 2. Chain length distributions for the experiment with two initial carbon sources and disturbances.

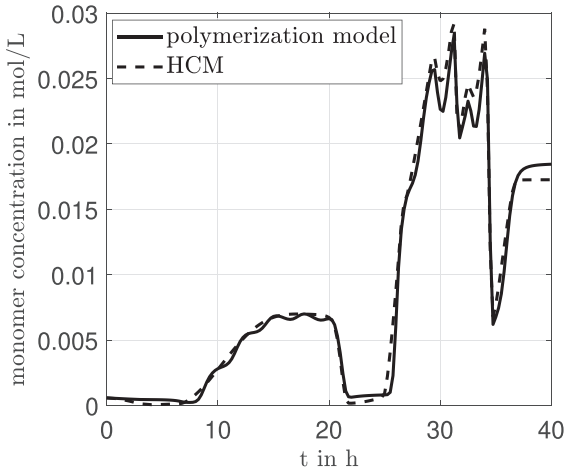

Fig. 3. Total monomer concentration of all chain lengths based on polymerization model and HCM.

was used in the polymerization approach (Eq. (20)). The parameters of the PI controller were set for the simulations in a way that the conservation of mass is fulfilled as precisely as possible. This is particularly challenging when abrupt changes in the process setup are present, e.g., in the present setting due to the pulses with ammonium chloride. The performance of the controller with regard to the conservation of mass of the two models is shown in Fig. 3.

4.2. Polymer chain length dynamics

With the polymerization model, chain length distributions can be simulated, evaluated at different times (Fig. 2) and their characteristic values can be determined (Fig. 4). The characteristic quantities presented in this article are number average MW, weight average MW and the PDI.

Focusing on the chains' MW, one can choose whether a certain time point is illustrated or the whole chain molecular weight dynamics in the 3D plot is shown (Fig. 2a and b). Characteristic time points were selected in Fig. 2a. If one compares the selected distributions at 12 h with the corresponding molar PHB concentrations of the model (Fig. 3), it can be seen that the shown distribution at 12 h is in the first PHB production phase. The PHB production in this phase is an interesting phenomenon, which can also be seen in the experimental data and thus, provides an indication that the cellular polymerases were already synthesized and active,

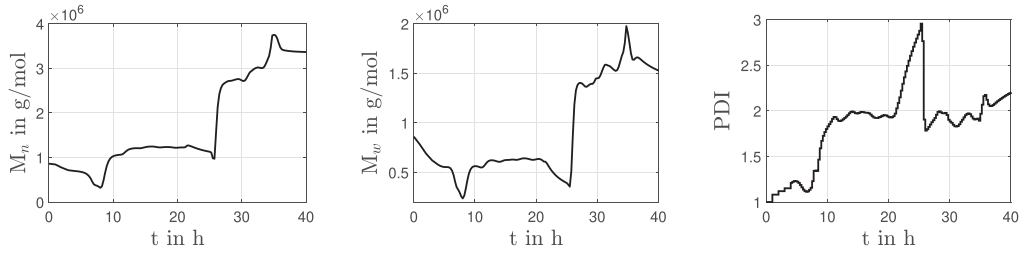

(a) Number average MW (b) Weight average MW (c) Polydispersity index

Fig. 4. Characteristic values of the distribution from the model data using fructose and acetic acid as carbon sources.

although there was still sufficient amount of ammonium chloride in the medium. Acetate was the preferred substrate in this first phase (Fig. 1). The characteristic values shown in Fig. 4 correspond to the literature values from PHB (Sudesh et al., 2000; Brandl et al., 1990; Peña et al., 2014).

According to the definition provided in Peña et al. (2014), the produced PHB belongs to "polymers with ultra high molecular weight", which is characterized by a tensile strength that is above the usual value of polypropylene. The peak in the CLD at 12 h at a molecular weight of approx. 2.1 10^5 g/mol is probably due to the initial distribution for active polymers (LP) shown in Appendix Fig. C.1, which has not been completely degraded by the depolymerases at this point. After another 4.5 h, i.e. after a process time of 16.5 h, the maximum PHB concentration in the first plateau is reached. The maximum of the distribution has increased and the peak of the starting population has disappeared. Except for a slight broadening of the population (Fig. 2b), the properties of the distribution have not changed significantly. With the distribution at 24 h, a snapshot was recorded showing the PHB minimum between the two increases. At this time point, the distribution is very disperse (PDI approximately 3), since all chains were degraded simultaneously and thereby, the weight average MW initially decreases significantly more than the number average MW. Further selected time points show the state at PHB concentration maximum at 31.25 h and the state after degradation at 34.75 h after a shot with fructose and nitrogen (see Figs. 1 and 3). The distribution after degradation shows higher molecular weight chains, which makes the distribution appear unsymmetrical. Compared to the previous distributions, the last distribution at 40 h has more polymer chains that are larger than 10^6 g/mol. From this, it can be concluded that the repeated polymerization and breakdown of polymer chains facilitates the formation of high molecular weight PHB. If one aims at monodisperse distributions (small PDI), which could be a desirable production goal due to the broad options in various process applications, one should refrain from such process control strategies.

4.3. Computational study: effects of different CN ratios and DO levels

With the developed HCM approach it is possible to evaluate different CN ratios with different oxygen availability, since biomass growth was related to the DO level (Eq. (6)) as investigated in Duvigneau et al. (2021b). Fig. 5 of this contribution shows three selected curves, one for an aerobic DO of 70%, an O_2 availability of 20% and a quasi-anaerobic process setting with 0.1% DO. The value of 20% DO was chosen by comparison with the investigation presented in Chatzidoukas et al. (2013), where the maximum PHB content for different DOs was investigated experimentally. In the present simulation study, the following can be stated:

- The smaller the dissolved oxygen, the more PHB can be formed after 120 h with the corresponding initial substrate concentrations.
- With lower oxygen availability, the ammonium chloride concentration can be reduced accordingly, so that more carbon is available for the accumulation of PHB. The optimal ratio depends on the DO, since the availability of oxygen has a strong influence on the biomass production.

With the two adjustable screws, an optimal balance between non-PHB biomass formation, which is essential for accumulation, and PHB accumulation can be found. Chatzidoukas and coworkers investigated this with another *Cupriavidus necator* strain (Chatzidoukas et al., 2013): Therein, the ammonium sulfate concentration (nitrogen source) was varied and the availability of carbon remained the same, a similar dynamics as shown in our Fig. 5 was found. Our results differ in the influence of the availability of oxygen: In Chatzidoukas' article, a clear optimum can also be found here at approx. 20% DO, while our model achieves even higher PHB concentrations with decreasing DOs (Chatzidoukas et al., 2013). On the one hand, this can be due to the different strains; on the other hand, our model is simplified to the extent that the formation of anaerobic metabolic products (succinate, fumerate, etc.) were not taken into account. In future work, the model prediction should be validated experimentally.

Due to the coupling of the HCM with the polymerization model it is now possible to evaluate not only the PHB concentration at a certain time point, it also allows to calculate the CLD and its characteristic values (Figs. 6–9). The Figs. 6–8 show weight average MW, number average MW and PDI for the CN ratios marked in Fig. 5 and the respective DOs: 70%, 20% and 0.1%. Independent of the DO, a dependency on the CN ratio can be seen in Figs. 6–8: A decrease of the CN ratio resulted in higher number average MW and weight average MW at 120 h. Further, it can be stated, that regardless of the oxygen supply and CN ratio, the PDI value is at approximately 2, which is typical for PHB (Sudesh et al., 2000). If the results of the different DOs are compared with another, the values for number average MW and weight average MW increase the less oxygen is available. Fig. 9 shows the dynamics of the CLD over the molecular weight of the chains and time. Here, the PHB accumulation begins later, the higher the DO and the lower the CN ratio is set. This effect can be explained from a biological point of view as follows: Due to a high availability of oxygen and a higher ammonium concentration, more carbon can be converted into non-PHB biomass over a longer time frame. Enough biomass is required to accumulate a sufficient amount of PHB. However, this is a sensitive balance that can be carefully investigated using the model presented here. With the help of the polymerization kinetics one reduces not only the amount of necessary bioreactor experiments to find the optimal DO and CN ratios, but also time and cost-intensive analysis, such as the evaluation of the polymer produced by using e.g. size exclusion chromatography.

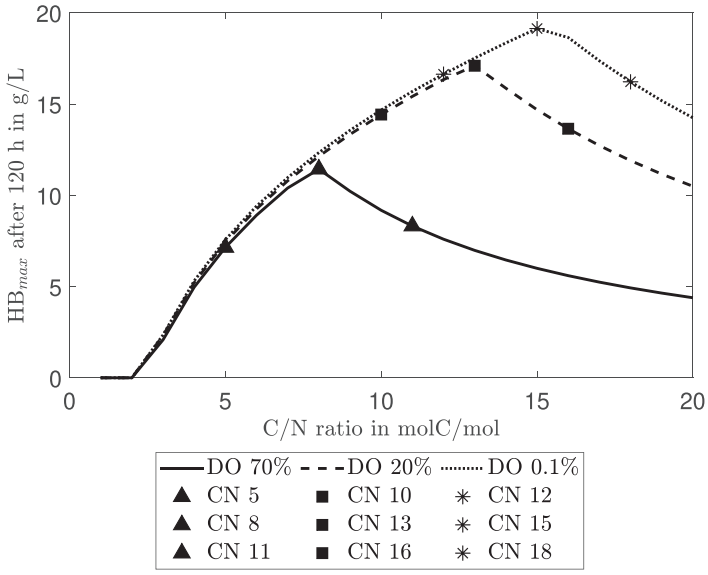

Fig. 5. Maximum PHB concentration in dependency of the initial carbon to ammonium (CN) ratio for three dissolved oxygen concentrations. For the simulation, we chose three CN ratios for each DO value (triangles, squares, asterisks).

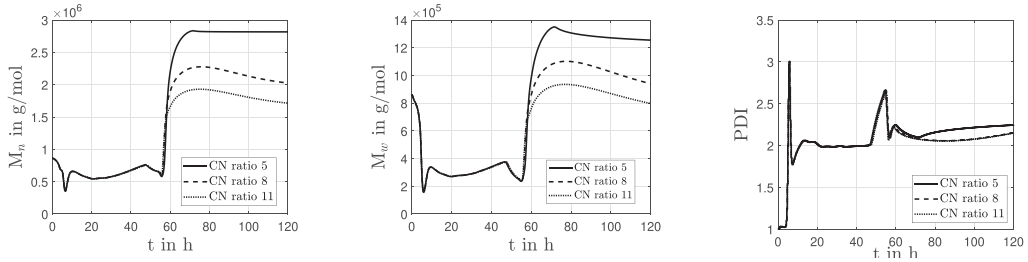

(a) Number average MW (b) Weight average MW (c) Polydispersity index

Fig. 6. Characteristic values of the distribution using a DO Level of 70% and different carbon to ammonium (CN) ratios.

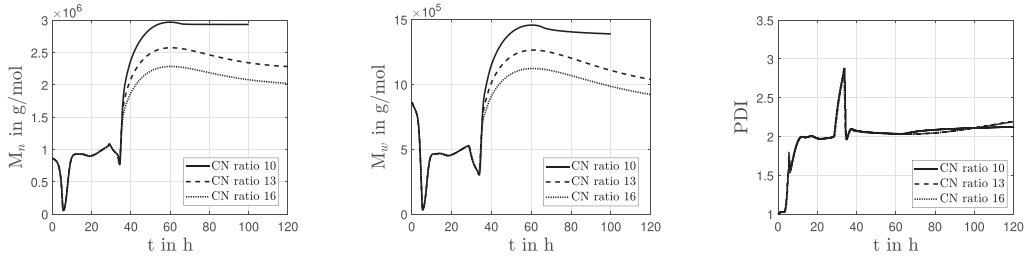

(a) Number average MW (b) Weight average MW (c) Polydispersity index

Fig. 7. Characteristic values of the distribution using a DO Level of 20% and different carbon to ammonium (CN) ratios.

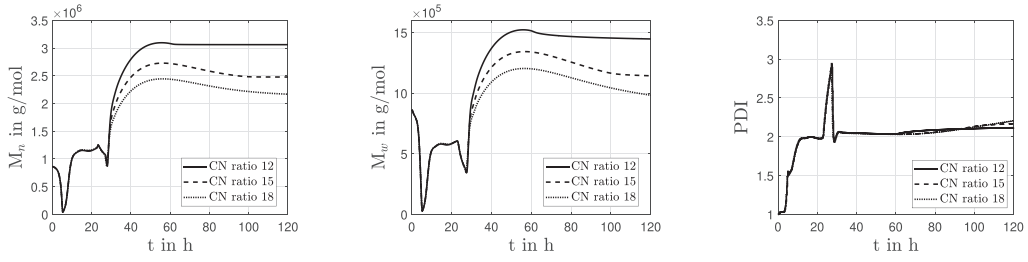

(a) Number average MW (b) Weight average MW (c) Polydispersity index

Fig. 8. Characteristic values of the distribution using a DO Level of 0.1% and different carbon to ammonium (CN) ratios.

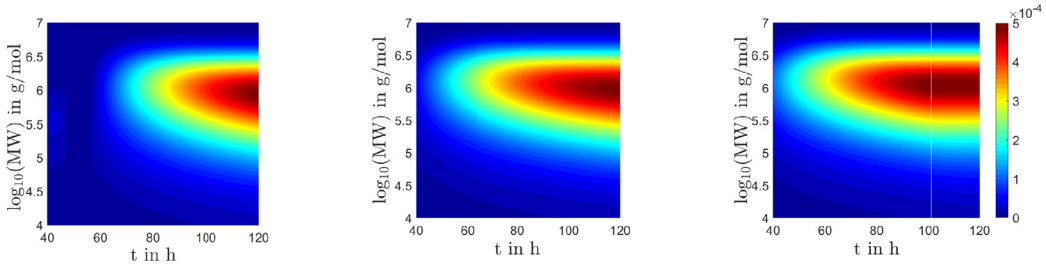

(a) 70% DO + CN ratio 8 (b) 20% DO + CN ratio 10 (c) 0.1% DO + CN ratio 15

Fig. 9. Dynamic behavior of chain length distribution applying different DOs and optimal CN ratios (see Fig. 5).

5. Conclusion

Multiscale modeling including metabolic information and polymerization kinetics represents an important step towards tailor-made biopolymers. The approach presented in this work couples an HCM with a polymerization model and thus, can describe not only the yields but also the CLD dynamics. The CLD provides important information about the properties of the polymer. In the present article the CLD dynamics of PHB production with fructose and acetate as carbon sources was simulated. The results have shown that, among other things, cyclic polymerization and degradation of PHB is useful to increase the final average molecular weight of the polymer chains. If one compares the average MW with data from the literature, it can be concluded that some properties (e.g. tensile strength) are similar to those of polypropylene (Peña et al., 2014).

In addition to the simulation of the CLD from the experiment with fructose and acetate, a simulation study with different CN ratios and DO levels was carried out. Here, the following can be concluded: The smaller the DO selected, the more PHB could be produced with a simultaneous decrease of the initial nitrogen concentration. The evaluation of the characteristic values of the CLD shows that the mean molecular weights at high CN ratios (small ammonium chloride concentrations) are smaller than at lower CN ratios, assuming the constant DO level for both. Finally, the following general statement can be made: The final process settings depend on the requirements with respect to the yield and the quality of the polymers.

Future work will deal with extension of the presented model for copolymer production. A recently developed model describing copolymer PHBV production considering exhaust CO_2 provides an excellent starting point (Duvigneau et al., 2021a). Further focus will be on estimation of kinetic parameters from the polymerization kinetics using own experimental data. In addition to the pure model formulation, direct relation of biopolymer composition and CLD on the one hand and physical as well as chemical properties of the product polymers on the other hand are still an open field and require deeper research efforts. Extended model formulation may result in multi-dimensional population balance equations which require tailored efficient solution methods (Dürr et al., 2017).

Declaration of Competing Interest

The authors declare that they have no known competing financial interests or personal relationships that could have appeared to influence the work reported in this paper.

CRediT authorship contribution statement

Stefanie Duvigneau: Conceptualization, Methodology, Software, Formal analysis, Investigation, Data curation, Visualization, Writing – original draft. **Robert Dürr:** Conceptualization, Methodology, Software, Formal analysis, Supervision, Writing – original draft. **Michael Wulkow:** Methodology, Software, Writing – original draft. **Achim Kienle:** Resources, Supervision, Funding acquisition, Writing – review & editing.

Acknowledgments

We would like to acknowledge the EU-programme ERDF (European Regional Development Fund) for funding the project DIGIPOL (ZS/2018/11/95489). We would like to thank Annette Wilisch–Neumann, Lena Kranert and Johannes Pohlodek for the support in laboratory. Furthermore, we would like to thank Lena Kranert for careful reading of the manuscript and giving helpful comments.

Appendix A. Metabolic model

No.	Reaction
1	FRU + PEP + ATP ⟶ F16P + PYR + ADP
2	F16P ⟶ F6P
3	F16P ⟷ 2 G3P
4	AMC ⟶ NH_3
5	G6P + 2 NADP ⟶ Rl5P + CO_2 + 2 NADPH
6	Rl5P ⟷ R5P
7	Rl5P ⟷ X5P
8	X5P + R5P ⟷ S7P + G3P
9	S7P + G3P ⟷ E4P + F6P
10	X5P + E4P ⟷ G3P + F6P
11	F6P ⟷ G6P
12	G3P + NAD + ADP ⟷ 3PG + NADH + ATP
13	3PG ⟷ PEP
14	PEP + ADP ⟷ PYR + ATP
15	OXA + ATP ⟷ PEP + ADP + CO_2
16	PYR + NAD ⟷ AcCoA + NADH + CO_2
17	AcCoA + OXA ⟷ ISC
18	ISC + NADP ⟷ αKG + NADPH + CO_2
19	αKG + NAD ⟶ SucCoA + NADH + CO_2
20	SucCoA + ADP ⟷ SUC + ATP
21	SUC ⟶ SUCx
22	SUC + FAD ⟷ MAL + FADH
23	MAL + NAD ⟷ OXA + NADH
24	MAL + NADP ⟷ PYR + CO2 + NADPH
25	PYR + ATP ⟶ OXA + ADP
26	ISC ⟶ SUC + GOX
27	AcCoA + GOX ⟶ MAL
28	NH_3 + αKG + NADPH ⟷ GLU + NADP
29	GLU + NH_3 + ATP ⟷ GLN + ADP
30	2 AcCoA ⟷ AcAcCoA
31	AcAcCoA + NADPH ⟶ HB + NADP
32	ACE + ATP ⟷ AcCoA + AMP
33	HB + NAD ⟷ AcACE + NADH
34	ACE + SucCoA ⟷ AcAcCoA + SUC
35	AcACE + ATP ⟶ AcCoA + AMP
36	2 NADH + O_2 + 4 ADP ⟶ 2 NAD + 4 ATP
37	ATP + AMP ⟷ 2 ADP
38	2 FADH + O_2 + 2 ADP ⟶ 2 FAD + 2 ATP
39	0.21 G6P + 0.07 F6P + 0.9 R5P + 0.36 E4P + 0.13 G3P + 1.5 3PG + 0.52 PEP + 2.83 PYR + 3.74 AcCoA + 1.79 OXA + 8.32 GLUT + 0.25 GLUM + 41.1 ATP + 8.26 NADPH + 3.12 NAD ⟶ BIO + 7.51 αKG + 2.61 CO2 + 41.1 ADP + 8.26 NADP + 3.12 NADH (Katoh et al., 1999)

Metabolite abbreviations

3PG	3-phosphoglycerate
αKG	alpha-ketoglutarate
ACE	acetate
AcACE	acetoacetate
AcAcCoA	acetoacetyl CoA
AcCoA	acetyl CoA
ADP	adenosine diphosphate
ATP	adenosine triphosphate
AMP	adenosine monophosphate
AMC	ammonium chloride
BIO	residual biomass
CO_2	carbon dioxide
E4P	erythrose-4-phosphate
F16P	fructose-1,6-bisphosphate
F6P	fructose-6-phosphate
FAD	flavin adenin dinucleotide, oxidized
FADH	flavin adenin dinucleotide, reduced
FRU	fructose
G3P	glyceraldehyde-3-phosphate
G6P	glucose-6-phosphate
GLN	glutamine
GLU	glutamate
GOX	glyoxylate
HB	hydroxybutyrate
ISC	isocitrate
MAL	malate
NAD	nicotinamide adenine dinucleotide (ox.)
NADH	nicotinamide adenine dinucleotide (red.)
NADP	nicotinamide adenine dinucleotide phosphate (ox.)
NADPH	nicotinamide adenine dinucleotide phosphate (red.)
NH_3	ammonia
O_2	oxygen
OXA	oxaloacetate
PEP	phosphoenol pyruvate
PYR	pyruvate
R5P	ribose-5-phosphate
Rl5P	ribulose-5-phosphate
S7P	sedoheptulose-7-phosphate
SUC	succinate
SucCoA	succinyl-CoA
SUCx	succinate, external
X5P	xylulose-5-phosphate

Appendix B. Hybrid cybernetic model

Table B.1
Values for the yields in g/gC of the matrix SZ subdivided into different subsections: substrates S_SZ (1), HB $S_{HB}Z$ (2) and total biomass S_xZ (3). Furthermore the normalized vector of uptaken carbon units $\mathbf{f_c}$ is shown.

AM	1	2	3	4	5	6	7	8	9	10	11
Y_{fru}	−2.50	−0.28	−2.50	−2.44	−0.40	−1.29	0.00	0.00	0.00	0.00	−2.50
Y_{ace} (1)	0.00	0.00	0.00	−0.06	−0.09	−1.19	−0.01	−2.46	−2.46	0.00	0.00
Y_N	−0.64	−0.73	0.00	−0.75	−0.50	0.00	−0.33	−0.51	0.00	−0.001	−0.77
Y_{HB} (2)	0.31	−1.59	1.19	0.00	−1.44	0.25	−1.78	0.00	1.19	−0.021	0.00
Y_c (3)	1.66	−0.05	1.19	1.58	−0.38	0.25	−1.08	1.08	1.19	−0.018	1.63
$\mathbf{f_c}$	1.00	0.75	1.00	1.00	0.83	0.99	0.72	0.98	0.98	0.01	1.00

Table B.2
Kinetic parameters for the hybrid cybernetic model.

Parameter	Unit	Value	Parameter	Unit	Value
estimated					
$k_{r,1}$	[1/h]	7.67×10^{-2}	$k_{r,7}$	[1/h]	1.451
$k_{r,2}$	[1/h]	8.85×10^{-1}	$k_{r,8}$	[1/h]	0.433
$k_{r,3}$	[1/h]	4.68×10^{-2}	$k_{r,9}$	[1/h]	0.426
$k_{r,4}$	[1/h]	8.79×10^{-2}	$k_{r,10}$	[1/h]	3.154
$k_{r,5}$	[1/h]	1.47×10^{-1}	$k_{r,11}$	[1/h]	0.197
$k_{r,6}$	[1/h]	6.16×10^{-1}			
fixed					
$\mathbf{k_e}$	[1/h]	$\mathbf{0.1}^{15x1}$			
$\boldsymbol{\alpha}$	[1/h]	$0.01\mathbf{k_e}$			
$\boldsymbol{\beta}$	[1/h]	$\mathbf{5}^{15x1}$			
K_N	[g/L]	0.01			
K_{FRU}	[g/L]	0.06			
K_{ACE}	[g/L]	0.03			
K_{HB}	[g/L]	0.05			

Appendix C. Polymerization model

Table C.1.

Table C.1
Parameters of the polymerization model.

Parameter	Unit	Value
k_{ini}	[1/h]	6.3×10^3
k_{m1}	[1/h]	1.1×10^4
k_{m2}	[1/h]	8.6×10^6
k_{term}	[1/h]	1.4
k_{deg}	[1/h]	83

Table C.2
Parameters of the controller (Eq. (20)).

Setting	K_P	Figure
CLD simulation/experiment	5	(2), (3), (4)
Different DO and CN ratios	1.3	(6), (7), (8), (9)

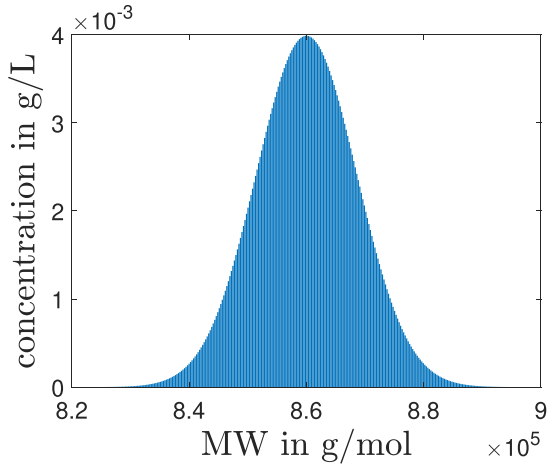

Fig. C.1. Normal distribution for the LP.

References

Brandl, H., Gross, R.A., Lenz, W.R., Fuller, R.C., 1990. Plastics from bacteria and for bacteria: poly (beta-hydroxyalkanoates) as natural, biocompatible, and biodegradable polyesters. Plastics from bacteria and for bacteria: poly ([l-hydroxy- alkanoates) as natural, biocompatible, and biodegradable. Adv. Biochem. Eng./Biotechnol. 41, 77–91. doi:10.1007/BFb0010232.

Bugnicourt, E., Cinelli, P., Lazzeri, A., Alvarez, V., 2014. Polyhydroxyalkanoate (PHA): review of synthesis, characteristics, processing and potential applications in packaging. Express Polym. Lett. 8 (11), 791–808. doi:10.3144/expresspolymlett.2014.82.

Chatzidoukas, C., Penloglou, G., Kiparissides, C., 2013. Development of a structured dynamic model for the production of polyhydroxybutyrate (PHB) in azohydromonas lata cultures. Biochem. Eng. J. 71, 72–80. doi:10.1016/j.bej.2012.11.015.

da Cruz Pradella, J.G., 2020. Economics and industrial aspects of PHA Production. In: Koller, M. (Ed.), The Handbook of Polyhydroxyalkanoates - Kinetics, Bioengineering, and Industrial Aspects. Taylor & Francis Group, pp. 389–404. doi:10.1201/9780429296635.

Dias, J.M., Serafim, L.S., Lemos, P.C., Reis, M.A., Oliveira, R., 2005. Mathematical modelling of a mixed culture cultivation process for the production of polyhydroxybutyrate. Biotechnol. Bioeng. 92 (2), 209–222. doi:10.1002/bit.20598.

Dürr, R., Bück, A., 2020. Approximate moment methods for population balance equations in particulate and bioengineering processes. Processes 8 (4). doi:10.3390/pr8040414.

Dürr, R., Duvigneau, S., Kienle, A., 2021. Microbial production of polyhydroxyalkanoates - modeling of chain length distribution. Comput. Aided Chem. Eng. 50, 1975–1982. doi:10.1016/B978-0-323-88506-5.50306-5.

Dürr, R., Müller, T., Duvigneau, S., Kienle, A., 2017. An efficient approximate moment method for multi-dimensional population balance models – application to virus replication in multi-cellular systems. Chem. Eng. Sci. 160, 321–334. doi:10.1016/j.ces.2016.11.015.

Duvigneau, S., Dürr, R., Behrens, J., Kienle, A., 2021. Advanced kinetic modeling of bio-co-polymer poly(3-hydroxybutyrate-co-3-hydroxyvalerate) production using fructose and propionate as carbon sources. Processes 9 (8). doi:10.3390/pr9081260.

Duvigneau, S., Dürr, R., Carius, L., Kienle, A., 2020. Hybrid cybernetic modeling of polyhydroxyalkanoate production in cupriavidus necator using fructose and acetate as substrates. IFAC PapersOnLine 53 (2), 16872–16877. doi:10.1016/j.ifacol.2020.12.1211.

Duvigneau, S., Dürr, R., Kranert, L., Wilisch-Neumann, A., Carius, L., Findeisen, R., Kienle, A., 2021. Hybrid cybernetic modeling of the microbial production of polyhydroxyalkanoates using two carbon sources. Comput. Aided Chem. Eng. 50, 1969–1974. doi:10.1016/B978-0-323-88506-5.50305-3.

Duvigneau, S., Kettner, A., Carius, L., Griehl, C., Findeisen, R., Kienle, A., 2021. Fast, inexpensive, and reliable HPLC method to determine monomer fractions in poly (3-hydroxybutyrate-co-3-hydroxyvalerate). Appl. Microbiol. Biotechnol. doi:10.1007/s00253-021-11265-3.

Franz, A., Song, H.S., Ramkrishna, D., Kienle, A., 2011. Experimental and theoretical analysis of poly(β-hydroxybutyrate) formation and consumption in Ralstonia eutropha. Biochem. Eng. J. 55 (1), 49–58. doi:10.1016/j.bej.2011.03.006.

Jiang, Y., Hebly, M., Kleerebezem, R., Muyzer, G., van Loosdrecht, M.C., 2011. Metabolic modeling of mixed substrate uptake for polyhydroxyalkanoate (PHA) production. Water Res. 45 (3), 1309–1321. doi:10.1016/j.watres.2010.10.009.

Katoh, T., Yuguchi, D., Yoshii, H., Shi, H.D., Shimizu, K., 1999. Dynamics and modeling on fermentative production of poly(β-hydroxybutyric acid) from sugars via lactate by a mixed culture of Lactobacillus delbrueckii and Acaligenes eutrophus. J. Biotechnol. 67 (2–3), 113–134. doi:10.1016/s0168-1656(98)00177-1.

Kegg pathway maps, 2020. Accessed: 2020-03 https://www.kegg.jp/kegg/pathway.html.

Kiparissides, C., 2004. Challenges in polymerization reactor modeling and optimization: a population balance perspective. IFAC Proc. Vol. (IFAC-PapersOnline) 37 (9), 137–154. doi:10.1016/s1474-6670(17)31805-0.

Koller, M., Braunegg, G., 2018. Advanced approaches to produce polyhydroxyalkanoate (PHA) biopolyesters in a sustainable and economic fashion. Euro Biotech J. 2 (2), 89–103. doi:10.2478/ebtj-2018-0013.

Koller, M., Horvat, P., Hesse, P., Bona, R., Kutschera, C., Atlić, A., Braunegg, G., 2006. Assessment of formal and low structured kinetic modeling of polyhydroxyalkanoate synthesis from complex substrates. Bioprocess Biosyst. Eng. 29 (5–6), 367–377. doi:10.1007/s00449-006-0084-x.

Krevelen, D., te Nijenhuis, K., 2009. Properties of Polymers : Their Correlation with Chemical Structure; Their Numerical Estimation and Prediction From Additive Group Contributions, vol. 4th. Elsevier Science. completely rev. ed. revised by K. te Nijenhuis

Lopar, M., Vrana Špoljarić, I., Atlić, A., Koller, M., Braunegg, G., Horvat, P., 2013. Five-step continuous production of PHB analyzed by elementary flux, modes, yield space analysis and high structured metabolic model. Biochem. Eng. J. 79, 57–70. doi:10.1016/j.bej.2013.07.003.

Mantzaris, N.V., Kelley, A.S., Daoutidis, P., Srienc, F., 2002. A population balance model describing the dynamics of molecular weight distributions and the structure of PHA copolymer chains. Chem. Eng. Sci. 57 (21), 4643–4663. doi:10.1016/S0009-2509(02)00370-6.

Mantzaris, N.V., Kelley, A.S., Srienc, F., Daoutidis, P., 2001. Optimal carbon source switching strategy for the production of PHA copolymers. AIChE J. 47 (3), 727–743. doi:10.1002/aic.690470319.

Metatool 5.1., 2019. Accessed: 2019-09-23 https://pinguin.biologie.uni-jena.de/bioinformatik/networks/.

Peña, C., Castillo, T., García, A., Millán, M., Segura, D., 2014. Biotechnological strategies to improve production of microbial poly-(3-hydroxybutyrate): a review of recent research work. Microb. Biotechnol. 7 (4), 278–293. doi:10.1111/1751-7915.12129.

Penloglou, G., Chatzidoukas, C., Kiparissides, C., 2012. Microbial production of polyhydroxybutyrate with tailor-made properties: an integrated modelling approach and experimental validation. Biotechnol. Adv. 30 (1), 329–337. Systems Biology for Biomedical Innovation. doi: 10.1016/j.biotechadv.2011.06.021.

Penloglou, G., Kretza, E., Chatzidoukas, C., Parouti, S., Kiparissides, C., 2012. On the control of molecular weight distribution of polyhydroxybutyrate in azohydromonas lata cultures. Biochem. Eng. J. 62, 39–47. doi:10.1016/j.bej.2011.12.013.

Penloglou, G., Roussos, A., Chatzidoukas, C., Kiparissides, C., 2010. A combined metabolic/polymerization kinetic model on the microbial production of poly(3-hydroxybutyrate). New Biotechnol. 27 (4), 358–367. doi:10.1016/j.nbt.2010.02.001.

Penloglou, G., Vasileiadou, A., Chatzidoukas, C., Kiparissides, C., 2017. Model-based intensification of a fed-batch microbial process for the maximization of polyhydroxybutyrate (PHB) production rate. Bioprocess Biosyst. Eng. 40 (8), 1247–1260. doi:10.1007/s00449-017-1784-0.

Pratt, S., Werker, A., Morgan-Sagastume, F., Lant, P., 2012. Microaerophilic conditions support elevated mixed culture polyhydroxyalkanoate (PHA) yields, but result in decreased PHA production rates. Water Sci. Technol. 65 (2), 243–246. doi:10.2166/wst.2012.086.

Ramkrishna, D., Song, H.-S., 2018. Cybernetic modeling for bioreaction engineering, vol. I. Cambridge University Press.

Riedel, S.L., Jahns, S., Koenig, S., Bock, M.C.E., Brigham, C.J., Bader, J., Stahl, U., 2015. Polyhydroxyalkanoates production with *Ralstonia eutropha* from low quality waste animal fats. J. Biotechnol. 214, 119–127. doi:10.1016/j.jbiotec.2015.09.002.

Roussos, A., Kiparissides, C., 2012. A bivariate population balance model for the microbial production of poly(3-hydroxybutyrate). Chem. Eng. Sci. 70, 45–53. doi:10.1016/j.ces.2011.07.049.

Sabapathy, P.C., Devaraj, S., Meixner, K., Anburajan, P., Kathirvel, P., Ravikumar, Y., Zabed, H.M., Qi, X., 2020. Recent developments in polyhydroxyalkanoates (PHAs) production—A review. Bioresour. Technol. 306, 123132. doi:10.1016/j.biortech.2020.123132.

Saliakas, V., Chatzidoukas, C., Krallis, A., Meimaroglou, D., Kiparissides, C., 2007. Dynamic optimization of molecular weight distribution using orthogonal collocation on finite elements and fixed pivot methods: an experimental and theoretical investigation. Macromol. React. Eng. 1 (1), 119–136. doi:10.1002/mren.200600015.

Satoh, H., Sakamoto, T., Kuroki, Y., Kudo, Y., Mino, T., 2016. Application of the alkaline-digestion-HPLC method to the rapid determination of polyhydroxyalkanoate in activated sludge. J. Water Environ. Technol. 14 (5), 411–421. doi:10.2965/jwet.16-027.

Scandola, M., Focarete, M.L., Frisoni, G., 1998. Simple kinetic model for the heterogeneous enzymatic hydrolysis of natural poly(3-hydroxybutyrate). Macromolecules 31 (12), 3846–3851. doi:10.1021/ma980137y.

Song, H.-S., Morgan, J.A., Ramkrishna, D., 2009a. Systematic development of hybrid cybernetic models: application to recombinant yeast co-consuming glucose and xylose. Biotechnol. Bioeng. 103 (5), 984–1002. doi:10.1002/bit.22332.

Song, H.-S., Ramkrishna, D., 2009. Reduction of a set of elementary modes using yield analysis. Biotechnol. Bioeng. 102 (2), 554–568. doi:10.1002/bit.22062.

Sudesh, K., Abe, H., Doi, Y., 2000. Synthesis, structure and properties of polyhydroxyalkanoates: biological polyesters. Prog. Polym. Sci. (Oxford) 25 (10), 1503–1555. doi:10.1016/S0079-6700(00)00035-6.

Tsang, Y.F., Kumar, V., Samadar, P., Yang, Y., Lee, J., Ok, Y.S., Song, H., Kim, K.H., Kwon, E.E., Jeon, Y.J., 2019. Production of bioplastic through food waste valorization. Environ. Int. 127 (April), 625–644. doi:10.1016/j.envint.2019.03.076.

Vale, H., McKenna, T., 2005. Modeling particle size distribution in emulsion polymerization reactors. Prog. Polym. Sci. 30 (10), 1019–1048. doi:10.1016/j.progpolymsci.2005.06.006.

Wang, J., Fang, F., Yu, H.Q., 2007. Substrate consumption and biomass growth of *Ralstonia eutropha* at various S0/X0 levels in batch cultures. Bioresour. Technol. 98 (13), 2599–2604. doi:10.1016/j.biortech.2006.09.005.

Wulkow, M., 2008. Computer aided modeling of polymer reaction engineering—The status of predici, I-simulation. Macromol. React. Eng. 2 (6), 461–494. doi:10.1002/mren.200800024.

Young, J.D., Ramkrishna, D., 2007. On the matching and proportional laws of cybernetic models. Biotechnol. Prog. 23 (1), 83–99. doi:10.1021/bp060176q.

Yu, J., Si, Y.T., 2004. Metabolic carbon fluxes and biosynthesis of polyhydroxyalkanoates in *Ralstonia eutropha* on short chain fatty acids. Biotechnol. Prog. 20 (4), 1015–1024. doi:10.1021/bp034380e.